
Computed Tomography of Hand and Wrist

Sri Priya Suresh and Tishi Ninan

Contents

1	Introduction	23
2	Computed Tomography Techniques	24
2.1	Patient Positioning.....	24
2.2	Technique.....	24
2.3	CT Arthrogram.....	24
3	Clinical Applications	24
3.1	Acute Trauma.....	24
3.2	Fractures of Carpal Bones.....	25
3.3	Fractures of Metacarpals.....	28
3.4	Dislocations.....	28
3.5	Fracture Union.....	29
3.6	Ligament Injury: CT Arthrography.....	30
3.7	Arthropathies.....	32
3.8	Tumor Imaging.....	33
4	Modern Advances	34
5	Conclusion	35
	References	35

Abstract

The use of computed tomography (CT) in imaging has expanded radically in the last four decades since its invention. Aided by advances in computing and engineering, it has grown from being an object of curiosity in research institutions to the main modality of medical imaging across the world. Although at present, the most common use of computed tomography with respect to imaging of the hand and wrist is in trauma; easy availability, high spatial resolution and recent innovations are helping it to break new ground in assessment of soft tissue structures and dynamic imaging.

1 Introduction

Computed tomography is becoming the mainstay of medical imaging. Several studies have validated this claim including the most recent report from National Council of radiation protection (NRCP) in the USA which stated that the number of CT studies has increased by 10 % per year from 1993 to 2006. Easy availability, very short scanning times and high spatial resolution are currently the main strengths of CT scanning. Modern advances in computing capability and digital image processing enabling instantaneous display of multi-planar reformats has helped to fuel the increase in demand in CT imaging for acute and chronic disorders. Moving on from diagnosis, CT is widely used for treatment planning and assessment of prognosis. Newer operating techniques and equipment enabling surgeons to operate on more complex injuries improving patient outcome also contributed

Sri P. Suresh (✉) · T. Ninan
Imaging Directorate, Department of Radiology,
Plymouth Hospitals NHS Trust, Derriford Road,
Crownhill, Devon, PL6 8DH, UK
e-mail: sureshpriya2000@yahoo.com

to increase use of CT for identification of even subtle injuries.

CT is pivotal in the imaging of hand and wrist. The unique configuration of the carpus, which involves complex articulation between multiple bones with different degrees of rotation and translation between them, makes accurate diagnosis of fractures and dislocations on two-dimensional images provided by plain radiograph problematic. For timely management of injuries and patient comfort, CT scan is the primary imaging modality of the wrist.

Modern multi detector row CT scans have the ability to produce slices that are a fraction of a millimeter thick thus providing spatial resolution capable of identifying non displaced fractures and tiny fracture fragments. CT can also be used to diagnose ligament injuries and arthritis especially in patients where MRI is difficult or contra-indicated.

2 Computed Tomography Techniques

2.1 Patient Positioning

For CT scans of the wrist and hand, the patient is asked to lie prone with the affected arm stretched out above his or her head with the hand and wrist placed with the palm facing down. This is often described as the ‘Superman’ position and it helps to reduce the dose delivered to the more radiosensitive parts of the body like cornea, breasts, mediastinum and abdominal organs. It also helps to reduce artifacts due to beam hardening that can occur if the hand is placed over the chest or by the side of the body for the scan.

2.2 Technique

Multiple rows of detectors are not essential for CT imaging of wrist trauma but they afford higher spatial and temporal resolution. Parameters like kV, mA, pitch and field of view are adjusted based on factors such as patient’s body mass index, presence or absence of cast and the indication for imaging. Radiation dose will be lower while imaging without a cast but in cases of unstable comminuted fractures or open injuries, cast and dressing can be left on. The patient is scanned in the “superman” position with

the wrist is in the middle of the gantry. The upper arm should be fully extended to counteract radial or ulnar deviation of the wrist. Excessive dorsal flexion of the wrist should also be avoided.

Technical parameters are set to achieve the highest spatial resolution but mindful of the radiation penalty. Newer dose and noise reduction techniques marketed by different manufacturers like Adaptive Statistical Iterative Reconstruction (ASiR) (GE) iDose (Philips), Adaptive Iterative dose Reduction (AIDR) (Toshiba) and Iterative Reconstruction in Image Space (IRIS) (Siemens) can be used according to local protocol.

Isotropic acquisition allows optimal reformation in multiple planes. Corrected transverse, sagittal, and coronal reformatted images are routinely obtained along the axis of the capitate bone.

Maximum bone detail is obtained by using high-resolution bone algorithms most of which involve edge enhancement.

2.3 CT Arthrogram

CT scanning of the wrist after injection of contrast is sometimes performed for better assessment of ligaments and joints in certain situations. Techniques and indications for this are discussed later in this chapter.

3 Clinical Applications

3.1 Acute Trauma

CT is now becoming the primary modality of cross sectional wrist imaging for trauma in several centres. Many centres still use MR as the preferred modality. In this chapter we shall consider the use of CT in various hand and wrist fractures.

3.1.1 Fractures of Distal Radius and Ulna

Fractures of the distal radius generate a high interest amongst orthopaedic and hand surgeons probably due to the fact that it is one of the most frequently encountered fractures in the emergency department. Treatment options have come a long way since the days of Colles’ landmark article on distal radius fractures where the main advice was to treat most patients non-operatively (Sternbach 1985). These days surgeons have more operative options and

Fig. 1 Radiograph of wrist demonstrating an intra-articular fracture at top left hand corner and clockwise images show coronal, transverse and sagittal CT reconstructions in the same patient. The degree of comminution and extent of articular depression is difficult to appreciate on the plain radiograph. Transverse section also demonstrates subluxation of the Distal radio ulnar joint (DRUJ) is difficult to appreciate on plain radiograph



expect information about fracture configuration, angulation and comminution to make decision about further management. The imaging parameters to be considered while evaluating distal radius fractures include radial inclination, radial shortening, radial tilt, articular incongruity and degree of comminution of fragments. Most of these parameters can be better identified on CT scans compared to plain radiographs. Although operative management of isolated distal ulnar fractures is less common, CT scan is occasionally indicated in badly comminuted, shortened fractures (Fig. 1).

3.2 Fractures of Carpal Bones

Wrist fractures are notoriously difficult to diagnose on initial radiographs. Various modalities including bone scintigraphy and MR imaging have been used in different institutions. There is a wide variation of

practice in the world in imaging of acute wrist injury. An international survey published in 2006 (Groves et al. 2006) of hospital practices revealed marked inconsistency in acute wrist fracture imaging protocols, which the authors believe are likely to be multifactorial but also probably reflected a deficiency in scientific evidence regarding the best practice for imaging occult wrist fractures. Moreover, practices will vary according to local expertise and availability of the different modalities operating within the constraints of individual healthcare local resources. In our institution we use CT scan to detect occult fractures if the second plain radiograph after 10–14 days of injury has been negative. Criteria for a bone fracture on CT images are the presence of a sharp lucent line within the trabecular bone, a break in the continuity of the cortex, a sharp step in the cortex, or a dislocation of bone fragments. Trabecular fractures on CT (without cortical disruption) can be difficult to differentiate from nutrient vessel. Soft tissue and

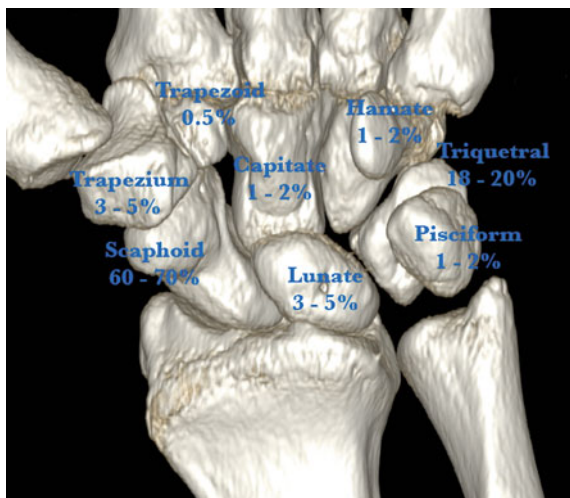


Fig. 2 Illustrates the relative frequency of fractures in the different carpal bones quoted by various sources

ligamentous injury on non-contrast CT cannot be accurately diagnosed (Adey et al. 2007). On MR imaging, one can more reliably identify trabecular fracture, and differentiation from a vessel can be done with much more confidence. In addition, bone bruising and ligamentous injuries can be more reliably identified on MRI and not CT. A recent meta-analysis (Yin et al. 2010) examined various studies performed in detecting occult scaphoid fracture comparing between bone scintigraphy, CT and MRI. MRI was shown to be more sensitive (96 %) than CT (93 %), but the specificity of both modalities remains the same (99 %). The meta-analysis also acknowledged that due to low numbers, there was lack of robust evidence to support one modality over another. (Fig. 2).

3.2.1 Scaphoid Fractures

The scaphoid is the largest bone of the proximal carpal row and provides an important link between the proximal and distal carpal row. It is also the most commonly fractured carpal bone accounting for about 70 % of wrist bone fractures (Welling et al. 2008). Waist of the scaphoid is the most common site of fracture.

Choice of imaging is dependent on local availability and as explained above, between MRI and CT, there is no clear winner. MRI is better in the diagnosis of trabecular fractures but CT is better in diagnosis of cortical fractures. MRI is more sensitive in early



Fig. 3 a Transverse CT section through scaphoid demonstrating fracture of the scaphoid waist. b Sagittal CT section through scaphoid demonstrating fracture of the scaphoid waist

diagnosis of fractures but there is no clear evidence that it is significantly better than CT (Yin et al. 2010).

The most commonly reported cause of scaphoid fracture is a fall on outstretched hand with forced dorsiflexion of the wrist. Compression or avulsion of the tuberosity is also seen occasionally. Proximal pole avulsion fractures can occur due to traction on the scapho-lunate ligament (Fig. 3).

3.2.2 Lunate Fractures

Lunate fractures account for about 4 % of all carpal fractures. Lunate occupies a central position in the proximal carpal row. Like the scaphoid, late diagnosis or non-diagnosis can result in carpal instability, nonunion and avascular necrosis. Isolated lunate fracture is often difficult to diagnose as lunate overlaps with other carpal bones on radiographs. CT imaging can demonstrate all patterns of fracture. Fracture pattern of the lunate is described according to anatomical location namely body (Fig. 4), dorsal pole and volar pole and also orientation of fracture line namely transverse and sagittal. Isolated fractures in the coronal plane are extremely rare.

3.2.3 Triquetral Fractures

Triquetral fractures are the second most common carpal fractures with a prevalence of about 20 %. Dorsal ridge fractures are the commonest and occur at the dorsal aspect due to impaction of ulnar styloid process against the dorsal surface during wrist

Fig. 4 **a** Plain radiograph that demonstrates a fracture of the lunate. **b** CT transverse section through the lunate in the same patient that demonstrates comminution that is difficult to appreciate on the plain radiograph

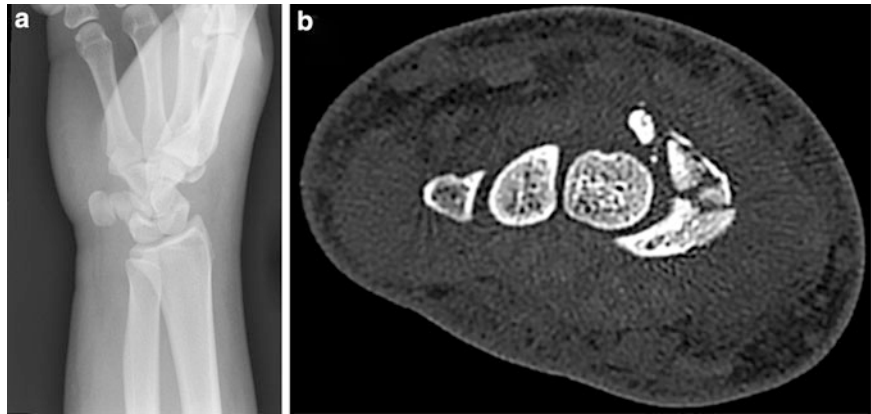


Fig. 5 CT transverse section through the triquetrum demonstrating a dorsal ridge fracture (*arrow*) that was occult on the initial plain radiograph

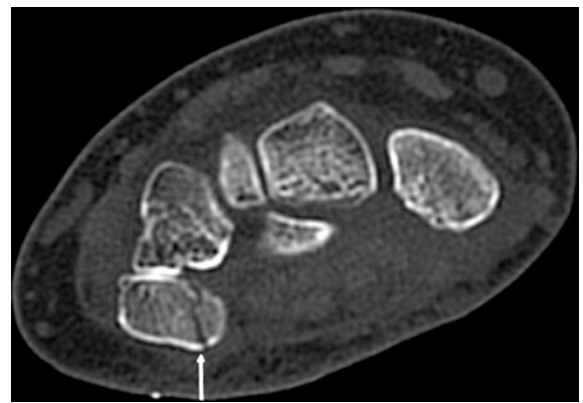


Fig. 6 CT transverse section demonstrating a minimally displaced fracture of the pisiform

hyperextension and ulnar deviation. Alternatively, dorsal ridge fractures may occur in hyperextension that results in ligamentous avulsion from the dorsal surface of the triquetrum. These fractures can be easily picked up on plain radiographs and CT is seldom indicated unless other associated injuries are present.

Fracture of the triquetral body is not very common and occurs in conjunction with perilunate dislocation and CT will be frequently indicated to assess the extent of the injury (Fig. 5).

3.2.4 Pisiform Fractures

The incidence of Pisiform fractures is about 2%. Pisiform fracture results from a direct blow. Presence of multiple ossification centres and overlap of other bones can make diagnosis of fracture on plain radiograph difficult and CT may be useful to explain the cause of symptoms (Fig. 6).

3.2.5 Trapezium and Trapezoid Fractures

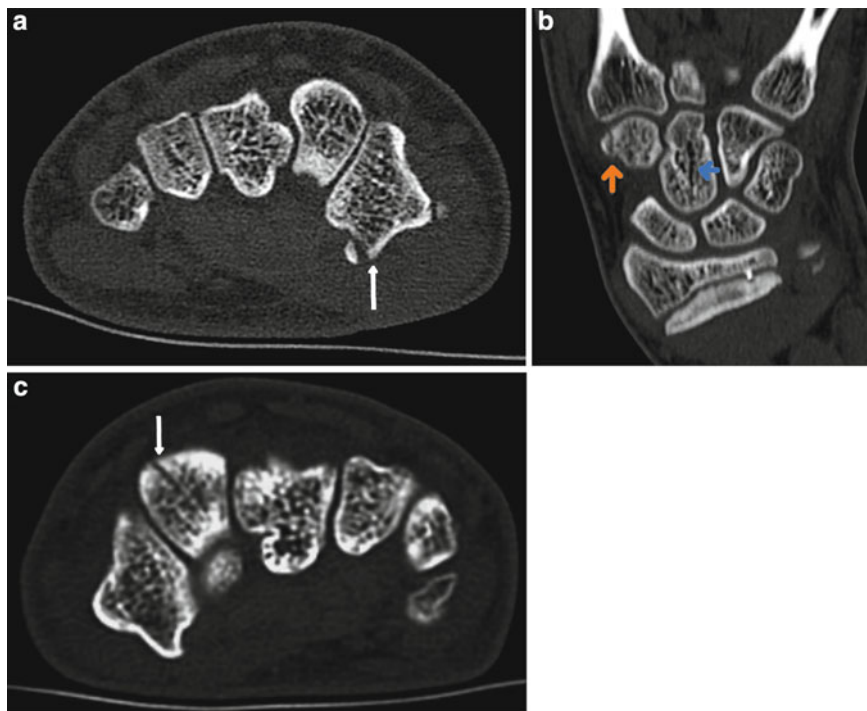
The trapezium is the most mobile bone of the distal carpal row. Trapezial ridge, a vertical prominence on the volar aspect of the trapezium where ligaments and the flexor retinaculum insert, is the most commonly fractured part of trapezium. It might be due to direct blow or avulsion.

Trapezoid is the least commonly fractured carpal bone and accounts for about 0.5% of carpal fractures. Mechanism is usually high energy impact and fractures can be associated with fractures of other bones. Even though fractures cannot be visualised on plain radiographs, they are frequently picked up on CT (Fig. 7).

3.2.6 Capitate Fractures

The capitate is the largest carpal bone. Injuries are usually caused by high-energy impact. The proximal third of the capitate is almost completely covered by

Fig. 7 **a** CT transverse section through the trapezium demonstrating a flake fracture (*arrow*). **b** CT coronal section demonstrating an undisplaced fracture of the trapezoid and a lucent line through the capitate representing a nutrient artery. **c** CT transverse section demonstrating a trapezoid fracture



articular cartilage and CT is frequently used to assess the involvement of the articular surface. Due to poor vascular supply, fractures of the capitate take longer to heal and CT is used to assess healing and look for signs of avascular necrosis (Fig. 8).

3.2.7 Hamate Fractures

Hamate fractures are frequently seen in sporting injuries in individuals using clubs or racquets e.g: Golf and Tennis. These fractures are usually subtle (particularly if they are through the hook of hamate) and are caused by direct trauma from the handle of the club or racquet and can be missed on the plain radiograph. Delayed diagnosis or malunion of the fracture can lead to ulnar nerve palsy and CT is helpful in this scenario (Fig. 9).

3.3 Fractures of Metacarpals

Although metacarpal shaft fractures are easily diagnosed on plain radiographs, fractures and fracture dislocations of the bases of metacarpals can be easily missed and lead to delayed diagnoses and increased morbidity in young patients. Even with views plain

radiographs can underestimate the comminution and angulation. Hence CT is used in diagnosis and operative planning of fractures of the metacarpal bones, especially comminuted fractures and those involving the articular surface. Fractures of the base of first metacarpal, even though relatively easier to see on plain radiographs frequently warrant further imaging to assess fragmentation and articular surface. These fractures, if not treated appropriately can lead to early osteoarthritis and disability (Fig. 10).

3.4 Dislocations

Dislocations of the carpal bones can be grossly classified into lunate dislocations, perilunate dislocations or mid-carpal dislocations based on the relative positions of the distal radius articular surface and the carpal bones. (Gilula and Minnie 1979).

In lunate dislocations, the lunate is displaced relative to the distal radius but the rest of the carpal bones (localized by the capitate) are centered over the distal radius. In peri-lunate dislocation, the lunate is centered over the distal radius but the rest of the carpal bones are displaced. If both lunate and capitate



Fig. 8 CT sagittal section through the Capitate demonstrating a fracture line in an oblique plain. (*blue arrow*) Compared with Fig. 7b, note that the line passes through two cortices indicating a fracture as opposed to a nutrient artery which seldom involves two cortices

are dislocated relative to the distal radius, the term mid-carpal dislocation is used.

CT scan is frequently used to assess collateral damage caused by lunate or perilunate dislocations. As stated earlier, CT is able to identify small flake fragments representing avulsion injuries and comminution, especially of articular surfaces although MR imaging is better at assessing ligament injuries. It is not uncommon to use both imaging modalities in conjunction in cases of significant trauma.

The most common dislocation is the perilunate dislocation. These are caused by high energy impact resulting in wrist hyper-extension and ulnar deviation. They are a broad continuum of injuries ranging from minor ligament strains to complete dislocation of the carpus. Perilunate dislocations are generally associated with carpal instabilities. On application of

stress, ligamentous failure occurs from ulnar side to radius (Fig. 11).

3.5 Fracture Union

As early as 1987, Bush et al. (1987) concluded that CT was much better than plain radiographs in the assessment of fracture union. CT is better fracture gaps, bony bridges and callus. Although literature has described use of MR and Ultrasound in assessing fracture union CT remains the test of choice in assessment of fracture healing, malunion and non union. Newer techniques discussed at the end of this chapter have improved the visualisation of cortical and cancellous bone even in the presence of metal work.

3.5.1 Sequelae of Trauma (Scapho Lunate Advanced Collapse and Scaphoid Non Union Advanced Collapse)

Degenerative changes in the joint are the most common sequelae of trauma.

Scapholunate Advanced collapse (SLAC) is caused by injury to the scapho lunate (SL) ligament, especially the dorsal component which is the most critical scapholunate stabiliser. The ligament can be injured in isolation or as part of perilunate dislocation.

When the SL ligament is injured, lunate tends to dorsiflex and scaphoid tends to rotate into a palmar flexed position. Capitate tends to follow the lunate into a dorsiflexed position and also migrates proximally. These spectrum of changes lead to a dorsal intercalated segmental instability (DISI) which in turn leads to degenerative changes commonly referred to as SLAC wrist.

Similar changes can also occur with nonunion of scaphoid fracture. The scapholunate ligament is usually intact but the biomechanics are similar to that described above. The degenerative changes in this case are usually referred to as Scaphoid Nonunion Advanced Collapse (SNAC). Pattern of degenerative changes can help to diagnose these conditions. Although MR arthrography is the preferred mode of investigation in several centres for this sort of injury, CT arthrography as described in the next section is almost as sensitive and can be used in places where MR arthrography is contraindicated or difficult to access.

Fig. 9 **a** and **b** Transverse and sagittal reconstructions demonstrating a fracture of the hook of the hamate

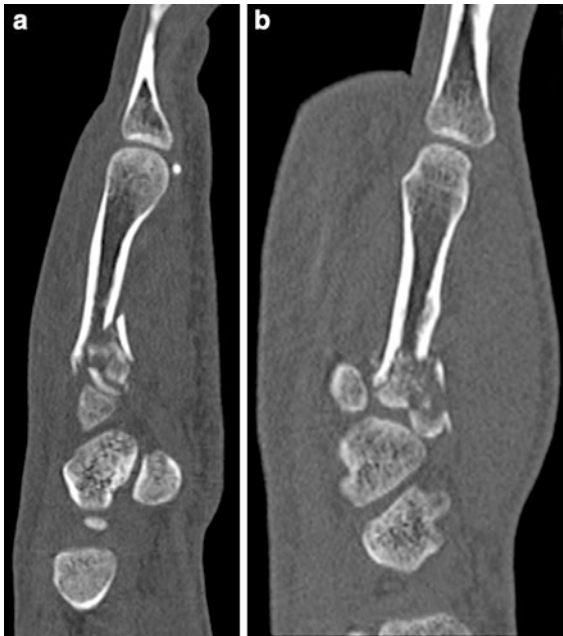
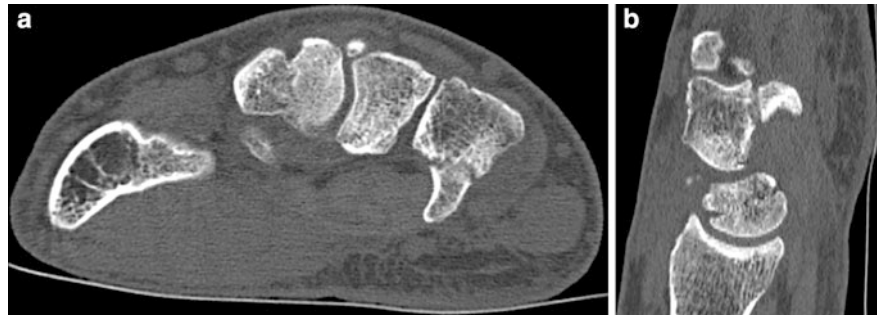


Fig. 10 Base of metacarpal fracture

First stage involves degenerative changes in the joint between radial styloid and the scaphoid. In the second stage degenerative changes progress to the whole radio-scaphoid joint. In the third stage, changes are seen in scaphocapitate or capitolunate joints (Fig. 12).

3.6 Ligament Injury: CT Arthrography

As alluded to before the wrist joint is one of the most complex joints in the body. For simplification it can be divided into three compartments. The distal radioulnar joint, the radiocarpal joint and the midcarpal joint.

The proximal carpal row is very important in the wrist movements as it acts as the intercalated segment

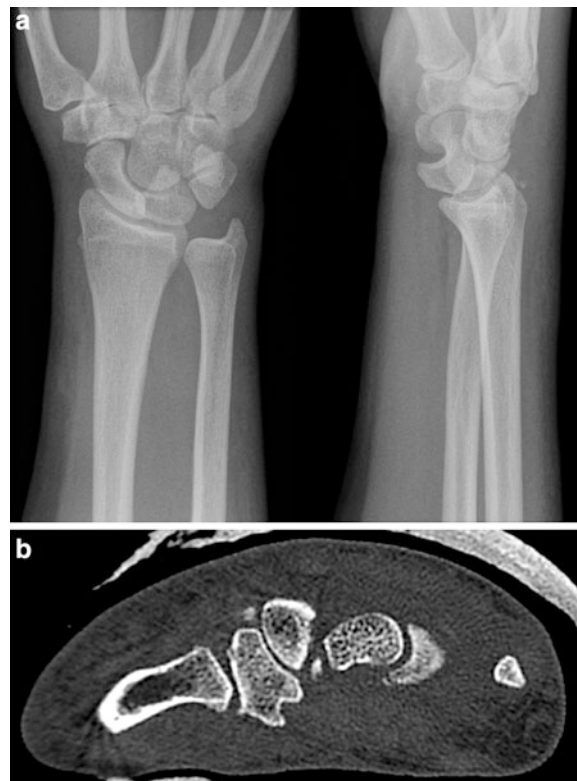


Fig. 11 Lunate dislocation with multiple small avulsion fractures better appreciated on CT scan

(Kauer 1980). The carpal bones in the proximal row are held together by the scapholunate (SL) and the lunotriquetral (LT) ligaments. Both these ligaments are horseshoe shaped, with the palmar and dorsal segments thicker (more important biomechanically) than the central segment (also known as proximal or membranous segment) (Boabighi et al. 1993) (Fig. 13).

They merge anteriorly and posteriorly with the articular capsule, and seal off the radiocarpal and midcarpal compartments (Berger 1996). Another

Fig. 12 **a** Demonstration of the normal SL angle (between 30° – 60°). **b** DISI deformity with dorsal tilt of lunate and SL angle $>60^{\circ}$

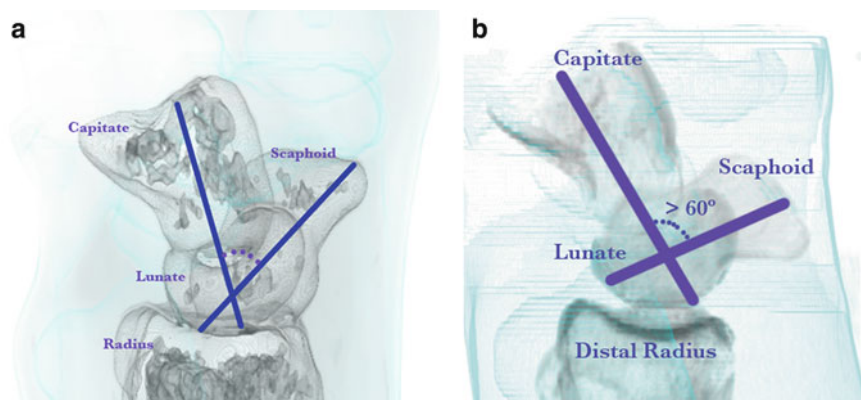
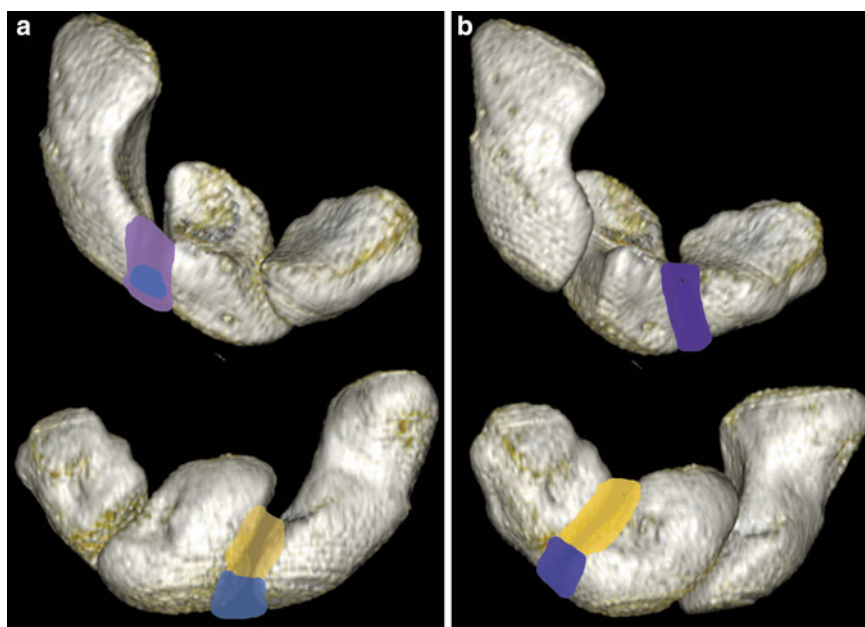


Fig. 13 Demonstration of intrinsic ligaments of the wrist. *Purple*: Volar scapho-lunate and luno triquetral ligaments. *Blue*: Proximal scapho-lunate and luno triquetral ligaments. *Yellow*: Dorsal scapho-lunate and luno triquetral ligaments



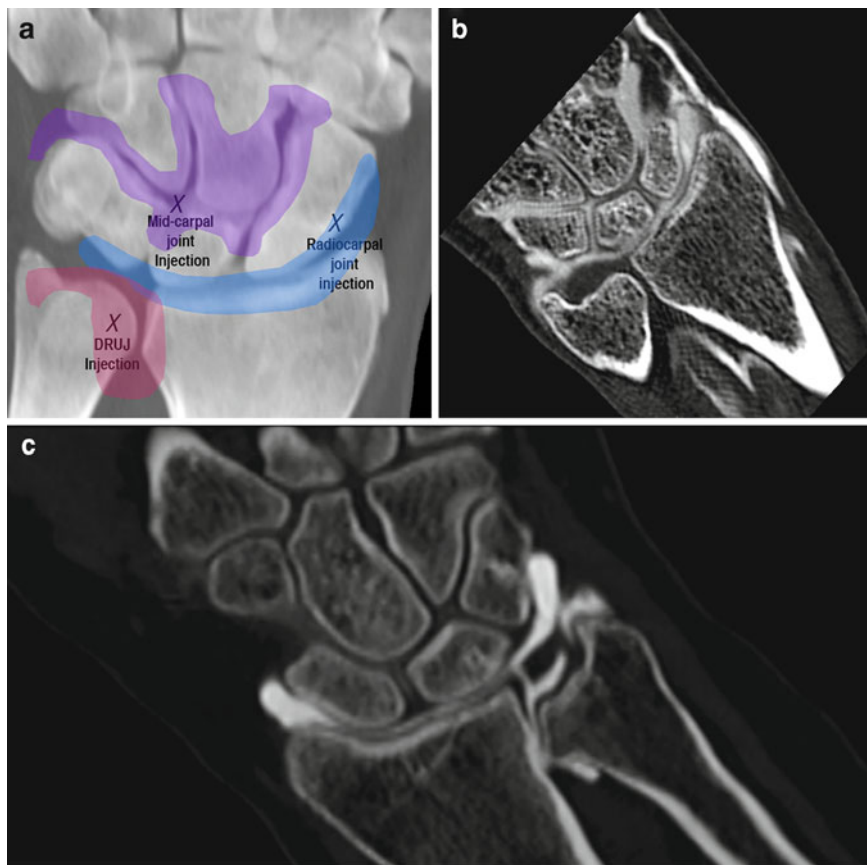
important structure is the Triangular Fibro Cartilage Complex (TFCC). It includes the extensor carpi ulnaris tendon sheath, the dorsal radioulnar ligament, the triangular fibrocartilage proper, the volar radioulnar ligament, the ulnocarpal ligaments, the ulnar collateral ligament, and the meniscus homologue. The TFCC is the key stabilizer of the DRUJ and it seals off the DRUJ from the radiocarpal joint. The capsular ligaments between the carpal bones form the secondary stabilizers of the wrist joint. These have been described in detail in literature. (Viegas 2001).

These intrinsic ligaments of the wrist can be depicted with several imaging modalities, including conventional arthrography, MR imaging (with and without intraarticular contrast agent administration),

and CT arthrography. The development of dynamic multislice CT studies allows a diagnostic approach that combines dynamic information and the accurate assessment of ligaments and the TFC complex.

Technique: Firstly the wrist is positioned horizontally under vertical fluoroscopic guidance. Then under aseptic conditions, using a 24-gauge needle, puncture is made on the dorsal aspect of the wrist (as demonstrated in Fig 14a). On average, a total of 5 mL of iodinated contrast medium is injected. The concentration should be lower than 300 mg of iodine per milliliter to avoid beam-hardening artifacts with MDCT. After the injection the patient is immediately directed to the MDCT to avoid excessive dilution of contrast medium.

Fig. 14 **a** Image representing the various joint capsules and sites for injection. *Purple*: mid carpal joint with injection site between the carpals *Blue*: Radiocarpal joint with preferred injection site being over the proximal articular surface of scaphoid. *Pink*: Distal radio-ulnar joint with preferred injection site over the distal ulna. **b** Contrast injected into radiocarpal joint was seen within the Distal radio ulnar joint (DRUJ) indicating a perforation of the Triangular fibro cartilage complex (TFCC). **c** Contrast is replacing the normal and LT ligaments indicating a full thickness tear in this young patient who had recent trauma



CT scan is then acquired as described in the previous section.

Coronal images provide a practical overview of the wrist joint. The central (proximal) parts of SL and LT ligaments are best seen on the coronal reformats and are usually meniscoid and insert onto cartilage. The transverse images are essential for appreciating the functionally important dorsal and volar portions of the SL and LT ligaments which are flat and insert onto the bones. Sagittal images provide a good analysis of the TFCC.

Ligament tears: These can be traumatic or degenerative. The traumatic tears are usually after fall on an outstretched hand and may be associated with carpal bone dislocations or fractures. Classification of ligament tears helps differentiate full-thickness (usually communicating) tears from partial-thickness (non-communicating) tears (Fig. 14b). For MDCT arthrography, a ligament tear is defined as communication of intraarticular contrast material through any segment of the ligament. TFCC tears (Fig. 14c) are

routinely classified according to the system developed by (Palmer 1989).

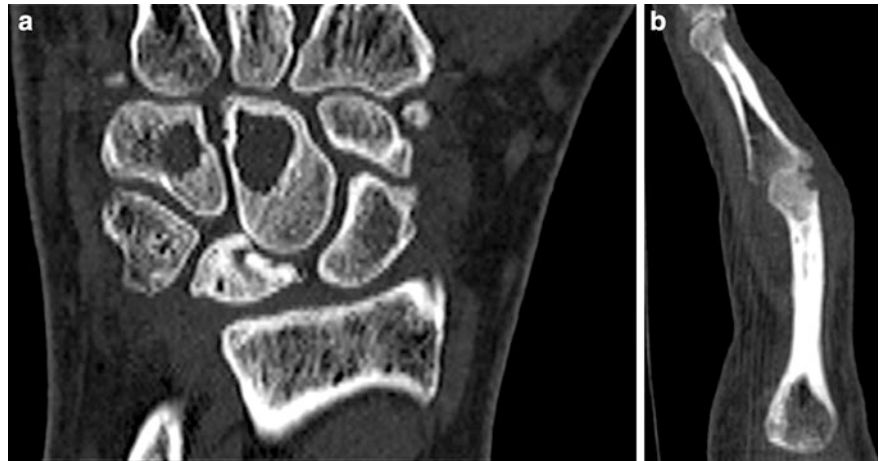
In the literature the sensitivity and specificity of CT arthrography has been described as high as 100 % for detecting SL ligament tears and 85 and 100 %, respectively, for LT ligament tears (Theumann et al. 2001; Schmid et al. 2005).

The advantages of CT are small field of view, excellent spatial resolution and quick scan time which virtually eliminates movement artifact.

3.7 Arthropathies

The commonest site of osteoarthritis (OA) in the hand is the first carpometacarpal (CMC) joint followed by distal interphalangeal joints. OA affecting the CMC joint is often debilitating, most commonly affecting postmenopausal women. The first CMC joint is the most commonly operated site in the hand for arthritis (Arnett et al. 1988). CT is useful in

Fig. 15 **a** Cyst within Capitate. Note the clarity of the intact cortical outline. **b** Erosion, tip of proximal phalanx. Due to the size of the erosion, it would have been difficult to illustrate on MR



operative planning and postoperative follow up if required.

Rheumatoid arthritis (RA) is a chronic inflammatory arthropathy of unknown etiology affecting a large cohort of the population. The success of disease modifying antirheumatic drugs (DMARD) and more recently the advent of biologic response-modifying drugs has increased the interest in the imaging modalities for evaluating the disease progression. These drugs are not only very expensive but are also potentially toxic necessitating their judicious use. The presence of erosions in early disease serves as a diagnostic marker for RA and is a sign of poor prognosis, signaling potentially aggressive disease (Van der Heijde et al. 1992).

Plain Radiographs, Doppler Ultrasound, Computerized Tomography (CT), Magnetic Resonance Imaging (MRI) and scintigraphy have been used for evaluation and diagnosis of the erosions. (Østergaard et al. 2003).

In CT cortical bone, being very dense, is readily visible, as is the interface with adjacent soft tissues. Thus, CT is capable of clearly delineating the borders of erosions and differentiating bone (whether edematous or not) from inflamed synovium. While plain radiography has traditionally been used as the gold standard for imaging erosions, the main disadvantage is that there are many regions such as the carpal bones where complex three-dimensional anatomy is very inadequately depicted using a two-dimensional modality. This problem is circumvented by multi-detector helical CT (MDCT), which offers the benefits of multiplanar capability, similar to MRI, with the enhanced cortical

definition intrinsic to plain radiography. Erosions on CT were defined as focal areas of loss of cortex with sharply defined margins, seen in two planes, with cortical break seen in at least one plane (Perry et al. 2005).

The main advantages of CT are that it is less expensive and faster than MR. The quick scan time is very useful in patients with concurrent shoulder disease, who have to be lying in the superman position for the scan. Another disadvantage of MR may be the conventional 3 mm slice thickness which can lead to partial volume artifacts on MR. This may lead to misinterpretation of small erosions. MDCT has the advantage of capability of acquiring images of 0.5 mm slice thickness thus reducing this artifact. Bone sclerosis can mask erosions on the MRI, but MDCT is capable of detecting erosions in the presence of extensive sclerosis. MRI does have the advantage that it allows imaging of inflammatory change within the joint, including synovitis, bone edema, and the “activity status” of erosions. None of these can be detected using CT (Perry et al. 2005). These modalities should therefore be regarded as complementary to each other in the detection of disease activity in rheumatoid patients (Fig. 15).

3.8 Tumor Imaging

Role of CT in evaluation of tumours can be complementary to MR, which is the main modality used for local tumor staging. If a lesion is suspected or discovered, the diagnostic work-up should begin with plain radiographs of the area of interest. If the tumor characterization with radiography is sufficient and in



Fig. 16 **a** Bone scintigraphy demonstrating a ‘hot spot’ which on subsequent CT. **b** was shown to be an osteoid osteoma with smooth round margins and central nidus. Contrast with **c** where

cortical break and irregularity of margins is demonstrated in keeping with a more aggressive lesion; in this case osteomyelitis

an adult metastatic disease is suspected then a bone scan to look for multiple metastatic lesions followed by a CT scan of the thorax, abdomen and pelvis is usually recommended. But if a primary bone tumor is suspected then work-up should proceed with MR imaging to evaluate the intra and extraosseous extent of tumor. Where it may be difficult to discern the pattern of bone destruction, it is recommended that CT be performed following radiography. This will help determine the pattern of bone destruction and periosteal new bone formation and to assess for the presence of matrix mineralization.

Osteoid osteoma is a benign bone tumor representing approximately 10 % of all benign bone tumors. It is more common in the lower limbs. Localization in the hand occurs with an incidence of 8 % of all reported cases (Allieu and Lussiez 1988). The phalanges are the most frequent sites in the hand (Ambrosia et al. 1987) followed by the carpal bones. Lesions in the hand may display less reactive sclerosis, a finding that can be misleading. Because of the proximity of the bones in the hands and feet, an inflammatory reaction that originates from one carpal or tarsal lesion often spreads to adjacent bones and joints. Moreover, soft-tissue swelling may be prominent in osteoid osteomas of the hands and feet, a finding that may resemble infection or inflammatory arthritis.

Many studies have shown CT is more useful than MR in illustrating the nidus. (Assoun et al. 1994) CT demonstrates the nidus as a round or oval well defined area with low attenuation. An area of high attenuation may be seen centrally, a finding that represents mineralized osteoid (Gamba et al. 1984) At radiography, it is very difficult to differentiate an intracortical abscess with a sequestrum and an osteoid osteoma with a calcified nidus. However, it is easier to differentiate between the two conditions on CT. In osteoid osteoma, the inner side of the nidus is smooth, and a round calcification is seen in the center of the nidus. In an intracortical abscess, the inner margin is irregular, and an irregularly shaped sequestrum is seen eccentrically (Chai et al. 2010) (Fig. 16).

4 Modern Advances

The limitations of CT scanning traditionally have been high radiation dose, low temporal resolution and artefacts due to metals. Another criticism has been that the anatomical images produced using a CT scanner are a ‘snapshot in time’ that do not show the dynamic interaction between the various structures which would be useful in guiding treatment. This is especially true of complex joints like the wrist.

Newer generation scanners have several features that help to overcome these limitations.

Various dose reduction techniques have been introduced by different CT manufacturers. With the increase in computing power, statistical and model based iterative reconstruction algorithms are being used for image manipulation. Research work being carried out in various hospitals including our institution have shown that extremity CT scans with good quality diagnostic images can be produced at doses comparable to plain radiography. If proven to work safely and accurately in a clinical setting, CT scans could replace plain radiography in the initial evaluation of trauma.

Modern scanners have high temporal resolution which can be utilised to perform dynamic imaging. Dynamic CT scan of the wrist has been performed in an experimental setting using cadaveric hand by Leng et al. (2011). This is possible due to the high temporal resolution offered by newer generation scanners. In the experimental setting, joint stability and relative motion of the carpal bones could be assessed. This is useful in early SLAC and SNAC wrist before the degenerative changes set in.

Artifacts due to metal can be reduced significantly by newer noise reduction techniques. Better receptors and high definition scanning modes also help to reduce metal artifacts. Another feature that is available in newer scanners is dual energy tubes. By using X-rays at two different energies (e.g 80 and 140 kV) metal prosthesis can be digitally subtracted to assess fracture healing, periprosthetic fractures and joint integrity.

Dual energy CT scanners have found application in characterisation of crystals in joints especially in patients suffering from Gout. Glazebrook et al. (2011) have demonstrated that Dual energy CT can successfully characterize uric acid crystals. Although in most clinical settings, it is difficult to justify irradiating the patient rather than aspirating easily accessible joints like the wrist, it can be used in special circumstances where aspiration is difficult or contra indicated.

5 Conclusion

In the four decades since its invention, the use of CT has rocketed. At the same time advances have placed it at the forefront of medical imaging. This progress looks set to continue and CT is more likely to become

the modality of choice in the imaging of trauma. Modern advances look promising and CT could encroach into the domain of other modalities like MR imaging and plain radiography.

References

- Adey L et al (2007) Computed tomography of suspected scaphoid fractures. *J Hand Surg* 32(1): 61–66. Available at <http://www.ncbi.nlm.nih.gov/pubmed/18780093>
- Allieu Y, Lussiez B (1988) Osteoid osteoma of the hand. Apropos of 46 cases. *Ann Chir Main* 7:298–304
- Ambrosia JM, Wold LE, Amadio PC (1987) Osteoid osteoma of the hand and wrist. *J Hand Surg (Am)* 12:794–800
- Arnett FC et al (1988) The American Rheumatism Association 1987 revised criteria for the classification of rheumatoid arthritis. *Arthr Rheum* 31(3):315–324. Available at <http://www.ncbi.nlm.nih.gov/pubmed/3358796>
- Assoun J, Richardi G, Railhac JJ et al (1994) Osteoid osteoma: MR imaging versus CT. *Radiology* 191(1):217–223
- Berger RA (1996) The gross and histologic anatomy of the scapholunate interosseous ligament. *J Hand Surg* 21(2):170–178. Available at <http://www.ncbi.nlm.nih.gov/pubmed/8683042>
- Boabighi A, Kuhlmann JN, Kenesi C (1993) The distal ligamentous complex of the scaphoid and the scapho-lunate ligament. An anatomic, histological and biomechanical study. *J Hand Surg Edinburgh Scotland* 18(1):65–69
- Bush CH, Gillespy T, Dell PC (1987) High-resolution CT of the wrist: initial experience with scaphoid disorders and surgical fusions. *Am J Roentgenol* 149(4):757–760
- Chai JW, Hong SH, Choi JY et al (2010) Radiologic diagnosis of osteoid osteoma: from simple to challenging findings. *RadioGraphics* 30:737
- Gamba JL, Martinez S, Apple J, Harrelson JM, Nunley JA (1984) Computed tomography of axial skeletal osteoid osteomas. *Am J Roentgenol* 142(4):769–772
- Gilula LA, Minnie A (1979) Review carpal injuries: analytic approach and case exercises. *Am J Roentgenol* 133: 503–517
- Glazebrook KN et al (2011) Identification of intraarticular and periarticular uric acid crystals with dual-energy CT: initial evaluation. *Radiology* 261(2):516–524. Available at <http://www.ncbi.nlm.nih.gov/pubmed/21926378>
- Groves AM et al (2006) An international survey of hospital practice in the imaging of acute scaphoid trauma. *Am J Roentgenol* 187(6):1453–1456. Available at <http://www.ncbi.nlm.nih.gov/pubmed/17114536>. Accessed 29 Jan 2012
- Kauer JM (1980) The functional anatomy of body mass. In: Damuth J, MacFadden BJ (eds) *Clin Orthop Relat Res* 149(149):9–20. Available at <http://www.ncbi.nlm.nih.gov/pubmed/11824284>
- Leng S et al (2011) Dynamic CT technique for assessment of wrist joint instabilities. *Med Phys* 38(S1):S50. Available at <http://link.aip.org/link/MPHYA6/v38/iS1/pS50/s1&Agg=doi>
- Østergaard M et al. (2003) New radiographic bone erosions in the wrists of patients with rheumatoid arthritis are

- detectable with magnetic resonance imaging a median of two years earlier. Available at <http://www.ncbi.nlm.nih.gov/pubmed/12905465>
- Palmer AK (1989) Triangular fibrocartilage complex lesions: a classification. *J Hand Surg* 14(4):594–606. Available at <http://www.ncbi.nlm.nih.gov/pubmed/2666492>
- Perry D et al (2005) Detection of erosions in the rheumatoid hand; a comparative study of multidetector computerized tomography versus magnetic resonance scanning. *J Rheumatol* 32(2):256–267. Available at <http://www.jrheum.org/content/32/2/256.abstract>
- Schmid MR et al (2005) Interosseous ligament tears of the wrist: comparison of multi-detector row CT arthrography and MR imaging. *Radiology* 237(3):1008–1013. Available at <http://www.ncbi.nlm.nih.gov/pubmed/16304116>
- Sternbach G (1985) Abraham Colles: fracture of the carpal extremity of the radius. *J Emerg Med* 2(6):447–450
- Theumann N et al (2001) Wrist ligament injuries: value of post-arthrography computed tomography. *Skelet Radiol* 30(2):88–93. Available at <http://dx.doi.org/10.1007/s002560000302>
- Van Der Heijde DM et al (1992) Prognostic factors for radiographic damage and physical disability in early rheumatoid arthritis. A prospective follow-up study of 147 patients. *Br J Rheumatol* 31(8):519–525. Available at <http://research.bmn.com/medline/search/results?uid=MDLN.92353764>
- Viegas SF (2001) The dorsal ligaments of the wrist. *Hand Clin* 17(1):65–75, vi. Available at http://www.ncbi.nlm.nih.gov/entrez/query.fcgi?cmd=Retrieve&db=PubMed&dopt=Citation&list_uids=11280160
- Welling RD et al (2008) MDCT and radiography of wrist fractures: radiographic sensitivity and fracture patterns. *Am J Roentgenol* 190(1):10–16. Available at <http://www.ncbi.nlm.nih.gov/pubmed/18094287>
- Yin Z-G et al (2010) Diagnosing suspected scaphoid fractures: a systematic review and meta-analysis. *Clin Orthop Relat Res* 468(3):723–734. Available at <http://www.pubmedcentral.nih.gov/articlerender.fcgi?artid=2816764&tool=pmcentrez&rendertype=abstract>